Published in final edited form as:
Toxicol Pathol. 2011 January ; 39(1): 220–233. doi:10.1177/0192623310389475.

An Approach to Experimental Synaptic Pathology Using Green Fluorescent Protein-Transgenic Mice and Gene Knockout Mice to Show Mitochondrial Permeability Transition Pore-Driven Excitotoxicity in Interneurons and Motoneurons

Lee J. Martin
Department of Pathology, Division of Neuropathology and the Pathobiology Graduate Program, and the Department of Neuroscience, Johns Hopkins University School of Medicine, Baltimore, MD, USA

Abstract

Researchers used transgenic mice expressing enhanced-green fluorescent protein (eGFP) driven by either the *glycine transporter-2* gene promoter to specifically visualize glycinergic interneurons or the *homeobox-9* (*Hb9*) gene promoter to visualize motoneurons for assessing their vulnerabilities to excitotoxins *in vivo*. Stereotaxic excitotoxic lesions were made in adult male and female mouse lumbar spinal cord with the specific *N*-methyl-*D*-aspartate (NMDA) receptor agonist quinolinic acid (QA) and the non-NMDA ion channel glutamate receptor agonist kainic acid (KA). QA and KA induced large-scale degeneration of glycinergic interneurons in spinal cord. Glycinergic interneurons were more sensitive than motoneurons to NMDA receptor-mediated and non-NMDA glutamate receptor-mediated excitotoxicity. Outcome after spinal cord excitotoxicity was gender-dependent, with males showing greater sensitivity than females. Excitotoxic degeneration of spinal interneurons resembled apoptosis, while motoneuron degeneration appeared non-apoptotic. Perikaryal mitochondrial accumulation was antecedent to both NMDA and non-NMDA receptor-mediated excitotoxic stimulation of interneurons and motoneurons. Genetic ablation of cyclophilin D, a regulator of the mitochondrial permeability transition pore (mPTP), protected both interneurons and motoneurons from excitotoxicity. The results demonstrate in adult mouse spinal cord that glycinergic interneurons are more sensitive than motoneurons to excitotoxicity that stimulates mitochondrial accumulation, and that the mPTP has pro-death functions mediating apoptotic and non-apoptotic neuronal degeneration *in vivo*.

Keywords

amyotrophic lateral sclerosis; apoptosis; cyclophilin D; excitotoxicity; green fluorescent protein; mitochondrial fission; synaptic pathology

Introduction

Synapses are the principal units of intercellular communication in neural circuits (Peters, Palay, and Webster 2001) and are highly vulnerable to many toxicants such as herbicides; pesticides; metals (e.g., lead, mercury, manganese, cadmium, iron, copper, and selenium); venoms; neurotransmitter receptor agonist/antagonist drugs; and inflammatory mediators,

Address correspondence to: Lee J. Martin, PhD, Johns Hopkins University School of Medicine, Department of Pathology, 558 Ross Building, 720 Rutland Avenue, Baltimore, MD 21205-2196; phone: 410-502-5170; fax: 410-955-9777; martinl@jhmi.edu.

including quinolinic acid (QA) and other naturally occurring excitotoxins (Verity 1997). Many of these agents can cause synaptic pathology, defined broadly as a perturbation in the function of synapses that results in transient or irreversible functional, biochemical, or structural abnormalities in the nervous system or end organs. The structural organization of a synapse consists of a presynaptic component (the axon terminal), a synaptic cleft (~20–40 nm in width), a postsynaptic component (a neuronal cell body or process, skeletal muscle cell, or organ cell), and a glial sheath (Peters, Palay, and Webster 2001). Each of these components has an elaborate structural organization and molecular composition. The presynaptic nerve terminal, containing several hundred neurotransmitter vesicles, is the principal site of regulated release of excitatory or inhibitory neurotransmitters through a process called the synaptic vesicle cycle (Sudhof 1995). The postsynaptic element contains many proteins that function in intercellular and intracellular signaling. These proteins are neurotransmitter receptors (ionotropic and metabotropic receptors); non-ligand-gated ion channels (Ca^{2+}, Na^{+}, K^{+}, and Cl^{-} channels); and other signal transduction molecules, including protein kinases, protein phosphatases, heterotrimeric GTP-binding proteins (G-proteins), phospholipases, nitric oxide synthase (NOS), calmodulin, and cytoskeletal proteins (Sotelo and Triller 1997). At the postsynaptic site, the postsynaptic density is an electron-dense meshwork of fine filaments that underlies the plasma membrane and is thought to anchor and cluster neurotransmitter receptors (Aarts and Tymianski 2004).

Many approaches are available to study synaptic pathology. Morphological approaches are standard, including electron microscopic and confocal microscopic analyses of presynaptic and postsynaptic compartments (Martin et al. 1994; Chang and Martin 2009). Neuroanatomical tract-tracing of pathways can be done to study connectivity after a toxic challenge (Siddiqui and Joseph 2005). Stereological determinations of synaptic markers can be made in specific brain regions (Calhoun et al. 1996). State-of-the-art approaches to study synaptic pathology in the context of anatomical systems can be done using magnetic resonance-diffusion tensor imaging (Stone et al. 2008). Biochemical determinations of synaptic markers and signal transduction can be made also, but these measurements often lack cellular resolution (Yang et al. 2010) unless laser capture microdissection of cells is performed (Ginsberg et al. 2006). Cell culture models can provide a venue to study the functional consequences of synaptic pathology by measurements of intra-cellular Ca^{2+}, free radical production, and mitochondrial membrane potential and Ca^{2+} uptake in real time (Nguyen et al. 2009). In cell culture settings, the mechanisms of excitotoxic synaptic pathology have been identified (Choi 1992; Carriedo et al. 1998) and continue to be studied with a focus on mitochondria (Yuan et al. 2007). This study illustrates how excitotoxic synaptic pathology can be studied *in vivo*.

Glutamate and aspartate are major excitatory neurotransmitters in the central nervous system (CNS) (Curtis, Phillis, and Watkins 1959; Watkins and Evans 1981). In normal circumstances, glutamatergic synaptic transmission occurs by regulated release of glutamate from presynaptic axon terminals. Concentrations of neurotransmitter glutamate at the synaptic cleft are estimated to be ~1 mM, whereas the concentration of interstitial glutamate is ~1 μM (Clements et al. 1992). At synapses, glutamate binds and activates several distinct molecular subtypes of glutamate receptors (GluRs) located on the plasma membranes of neurons and some glial cells (Nakanishi 1992; Seeburg 1993). These receptors are categorized as members of one of two families, the ionotropic (ion channel) receptors and G-protein coupled metabotropic receptors (Nakanishi 1992; Seeburg 1993). Ion channel GluRs are classified as the *N*-methyl-*D*-aspartate (NMDA) receptors and the non-NMDA receptors. The non-NMDA GluRs are further divided into the α-amino-3-hydroxy-5-methyl-4-isoxazole propionate (AMPA) and kainate (KA) receptors (Collingridge et al. 2009).

Excess synaptic glutamate can mediate excitotoxicity (Lucas and Newhouse 1957; Choi 1992; Olney 1994; Aarts and Tymianski 2004). Excitotoxicity is pathologic neurodegeneration mediated by excessive activation of non-NMDA and NMDA GluRs and also voltage-dependent ion channels (Choi 1992; Olney 1994). The excessive interaction of ligand with GluR subtypes causes pathophysiological changes in intracellular ion concentrations, pH, protein phosphorylation, energy metabolism, and mitochondrial function and movement (Choi 1992; Reynolds et al. 2004; Aarts and Tymianski 2004). When GluRs are stimulated, increased cytosolic free Ca^{2+} causes activation of Ca^{2+}-sensitive proteases, protein kinases/phosphatases, phospholipases, and NOS as well as Ca^{2+}uptake by mitochondria (Carriedo et al. 1998; Aarts and Tymianski 2004). The mitochondrial permeability transition pore (mPTP) is also involved in the pathobiology of excitotoxicity in cell culture models of glutamate exposure (Li, Brustovetsky, and Brustovetsky 2009) and glucose/oxygen deprivation (Malouitre et al. 2010). Several naturally occurring neurotoxic chemicals can bind and potently activate GluRs, including quinolinic acid, kainic acid, and domoic acid (Olney 1994). Thus, excitotoxicity has fundamental importance to clinically relevant neurotoxicology and synaptic pathology (Stewart et al. 1990) as well as several neurological disorders (Martin 2002). The expression of GluR subtypes is responsible in part for the high sensitivity or selective vulnerability of certain types of brain cells and synapses to excitotoxicity (Auer and Benveniste 1997; Martin 2002) but is insufficient to explain fully the phenomenon of selective vulnerability and cell death (Aarts and Tymianski 2004).

Selective vulnerability is a concept that refers to the phenomenon whereby an insult that affects the nervous system gives rise to damage to certain brain regions and types of cells (Auer and Benveniste 1997). The principal neurons within a CNS region have usually garnered much of the attention regarding excitotoxic selective vulnerability. Much less work has been devoted to interneurons and their vulnerability to excitotoxicity. This is particularly surprising when considering the function of interneurons in strongly modulating the excitability of principal neurons within their region (Miles 2000). This lack of attention is explained in part by the prior inability to specifically and unequivocally recognize neurotransmitter-identified cell bodies and processed of interneurons (Olvia et al. 2000). Traditional neurotransmitter antibody-based detection of interneurons has been problematic because the neuronal cell bodies of γ-aminobutyric acid (GABA)ergic, glycinergic, and glutamatergic interneurons usually remain unstained, and thus cannot be visualized, but presynaptic bouton labeling of GABAergic, glycinergic, and glutamatergic markers is robust (Olvia et al. 2000; Chang and Martin, 2009). The visualization of interneurons in tissue sections can be improved by methods requiring intracerebroventricular treatment of animals with colchicine or special tissue fixation approaches (Skirboll et al. 1989), but results based on these methods can be variable. The ability to genetically express jellyfish (*Aequorea victoria*) and coral fluorescent proteins in mammalian cells and in mice (Okabe et al. 1997) has revolutionized neuroscience and neurotoxicology. Under the control of specific gene promoters, fluorescent proteins can serve as reporters for cells and tissues (Okabe et al. 1997). Transgenic mice have been created that express enhanced green fluorescent protein (eGFP) in interneurons (Zeilhofer et al. 2005) or in motoneurons (Wichterle et al. 2002). Using these mice, my laboratory tested the hypothesis that excitotoxicity *in vivo* induces spinal interneuron cell death and mitochondrial accumulation that is antecedent to the cell death and mediated by the mPTP.

Materials and Methods

Transgenic and Null Mice

Adult (6–8 months old), transgenic (tg), and gene-targeted knockout (null) male and female mice were used. Transgenic mice expressed eGFP in subsets of interneurons or motoneurons. Glycine transporter-2 (GlyT2)-eGFP tg mice (Zeilhofer et al. 2005),

expressing *GlyT2* gene promoter-driven eGFP in glycinergic interneurons only, were derived originally from breeders generously provided by Dr. Hanns Zeilhofer (Institute of Pharmacology and Toxicology, University of Zurich, Switzerland). Breeder pairs of homeobox-9 (Hb9)-eGFP tg mice (stock # 005029) were purchased from The Jackson Laboratories (Bar Harbor, ME). These mice express eGFP driven by the *Hb9* gene promotor (Wichterle et al. 2002). Hb9 is a homeodomain transcription factor that is expressed by motoneurons and functions during development to consolidate motoneuron identity (Arber et al. 1999; Thaler et al. 1999). Two different lines of cyclophilin D (CyPD) null mice (knockout of the $ppif^{-/-}$ gene) were used: one line on a 129SV genetic background (Baines et al. 2005; Martin et al. 2009) and another line on a C57BL/6 genetic background (Basso et al. 2005). Control mice for the null experiments were age- and sex-matched 129SV and C57BL/6 wild-types. All mice were housed in a laboratory animal suite with an ambient temperature of 23° C, 12-hour light/dark cycle, and *ad libitum* access to food and water. Mouse care was provided in accordance with the National Institutes of Health *Guide for the Care and Use of Laboratory Animals*. The Animal Care and Use Committee of the Johns Hopkins University School of Medicine approved the animal protocol. Mouse cohort sizes for each experimental manipulation and data set were 6–10 mice per group.

High-Precision Excitotoxic Lesions in Mouse Spinal Cord

The mice were anesthetized deeply with isoflurane (4%) in O_2 in an induction chamber, and the lower back was shaved of fur and cleaned with betadine and 70% isopropyl alcohol. Mice were mounted in a stereotaxic apparatus (Stoelting, Wood Dale, IL) with a customized vertebral column stabilizer. Surgical anesthesia was maintained with isoflurane (2%), nitrous oxide (66%), and O_2 (32%) delivered by a nosepiece mask. Body temperature was maintained with external warming. A midsagittal incision (4 mm) was made over the lumbar back, and the dorsal part of the L1–L3 vertebral column was carefully freed of attached fascia and skeletal muscle. After a laminectomy at L2, performed slowly and carefully without traumatizing the spinal cord and causing any edema, a stereotaxic injection of the specific NMDA receptor agonist quinolinic acid (QA, 2.5 or 5 μmol, 1μl volume) or the non-NMDA ion channel GluR agonist kainic acid (KA, 400 μmol, 1μl volume) was made unilaterally directly into the parenchyma of lumbar spinal cord using a mounted 10-μl Hamilton syringe and a sharp, stainless steel needle (26 gauge) with a 45° beveled angle. QA and KA (Sigma, St. Louis, MO) were dissolved in 100 mM phosphate-buffered saline (PBS, pH 7.4) and were stored in the dark at −20° C until used. These doses of QA (2.5 or 5 μmol) and KA (400 μmol) were established empirically because they produced robust neuronal cell death with minimal fatality due to status epilepticus or cardiorespiratory arrest in female mice. However, it was determined here that these doses of QA could be fatal in male mice. Mice injected unilaterally with 100 mM PBS (1 μl) were controls. Injections were performed manually. To prevent leakage from the injection site, neurotoxin and buffer were injected over 1 min, and the needle was left in place for 3 min before it was withdrawn slowly. The laminectomy was sealed with softened W-31 bone wax (Ethicon, Somerville, NJ), and the wound was closed with a skin clip. Buprenorphine (0.2 mg/kg, subcutaneously, once immediately after surgery and 12 hours later) was used for postoperative analgesia. All animals recovered from the anesthesia.

At 4, 12, and 24 hours after the excitotoxic injection, mice were deeply anesthetized with an overdose of sodium pentobarbital and perfused intracardially with ice–cold PBS (100 mM, pH 7.4) followed by ice–cold 4% paraformaldehyde in PBS. After perfusion-fixation, spinal cords remained *in situ* for 2 hours before they were removed by dorsal laminectomy from the vertebral column. After the spinal cords were isolated and photographed, the lumbar enlargements were cryoprotected in 20% glycerol-PBS, and frozen under pulverized dry ice. Transverse, serial, symmetrical cryosections (40 μm) were cut using a sliding microtome

and stored individually in 96-well plates. Sections were selected with a random starting level and then systematically sampled (every 10th section) to generate a subsample of sections from each mouse lumbar spinal cord. Sections were mounted on glass slides, counterstained with the nuclear dye Hoechst 33258 (Invitrogen Molecular Probes, Carlsbad, CA), and were used for counting of eGFP-positive interneurons and motoneurons at 24 hours after excitotoxic lesioning.

Adjacent sections were used to detect, by fluorescence microscopy, cleaved caspase-3 as a marker for apoptosis (Lok and Martin 2002), and manganese superoxide dismutase (MnSOD) as a marker for mitochondria (Chang and Martin 2009). Antibodies to cleaved caspase-3 (Cell Signaling Technology, Beverly, MA) and MnSOD (Assay Designs-Enzo Life Science International, Plymouth Meeting, PA) were rabbit polyclonal. Secondary antibody was Alexa-594-conjugated goat anti-rabbit (Invitrogen Molecular Probes) for red signal detection. Sections were counterstained with the blue nuclear stain Hoechst 33258 before mounting on glass slides and cover-slipping with Antifade media (Invitrogen Molecular Probes). To confirm the mitochondrial staining patterns seen by immunofluorescence, MnSOD was also localized by immunoperoxidase staining using diaminobenzidine as the chromogen as described (Martin et al. 2007).

Counting eGFP-Positive Neurons in Lumbar Spinal Cord

Hoechst 33258-stained sections were used to count eGFP-positive neurons in spinal cord at 24 hours after the excitotoxic lesion or after PBS injection. Individual cell counts were not determined on the 4- and 12-hour survivors because previous work has shown that excitotoxic cell loss emerges between 12 and 24 hours (Lok and Martin 2002). The 4- and 12-hour mice were used for mitochondrial localization studies. eGFP-positive interneurons in GlyT2-eGFP mice were counted in the intermediate zone. eGFP-positive motoneurons in Hb9-eGFP mice were counted in the ventral horn. Counts of eGFP-positive neurons were made in systematically random sampled sections through the lumbar spinal cord of PBS-injected mice and KA-and QA-injured mice. Sections were selected with a random start and then systematically sampled (every 10th section) to generate a subsample of sections from each mouse. Green cell profiles were counted in the side ipsilateral to the excitotoxic lesion using an oil immersion lens (1,000×). Careful focusing through the z-axis of the sections was necessary to count profiles of interneurons and motoneurons with a blue nucleus throughout the depth of the section. Counts of eGFP-positive interneurons and motoneurons in spinal cord were compared using one-way ANOVA. When the *F*-value of the ANOVA was significant, the Newnan-Keuls multiple range test was used to identify significant differences among treatments. The level of statistical significance was set at $p < .05$.

Neurodegeneration Classification

Apoptotic cells were identified by the Hoechst staining pattern in the nucleus. An apoptotic cell was defined as a profile with a blue nucleus condensed into single or multiple round aggregates (Lok and Martin 2002). In cresyl violet-stained sections, neuronal degeneration was classified as apoptotic or non-apoptotic, including necrotic and continuum forms of cell death (Martin et al. 1998; Martin 2010), using specific criteria as described (Portera-Cailliau, Price, and Martin 1997a, 1997b; Martin et al. 1998; Martin 2010). Briefly, apoptotic cells were shrunken and round with a translucent rim of cytoplasm, detached from the surrounding neuropil, and with two or more sharply delineated, uniformly dense, smooth, round, regularly shaped discrete amalgamations of dark purple-stained chromatin. Non-apoptotic degenerating cells were distinguished by a swollen pale nucleus with a highly vacuolated or disintegrating cytoplasm (necrosis). Alternatively non-apoptotic dying cells had a nucleus with small to large, irregularly shaped, chromatin masses and an apparently intact plasma membrane with lower-amplitude cytoplasmic vacuolation than that seen in

necrotic cells. These degenerating cells would be classified as continuum or hybrid forms of cell death (Martin et al. 1998; Martin 2010).

Estimating Mitochondrial Content in Lumbar Spinal Cord Neurons

MnSOD immunofluorescence was used to estimate the abundance of mitochondria in GlyT2-eGFP and Hb9-eGFP neurons after excitotoxin or PBS injection into spinal cord. Using a Zeiss Axiophot epifluorescence microscope, neurons were identified as green, and then discrete red fluorescent MnSOD-positive particles were imaged in the z-axis approximately at the neuron center as judged by the blue nucleus. For each mouse, ~25 eGFP-positive neuron profiles were assessed in the intermediate zone or ventral horn. MnSOD immunostaining fluorescence intensity was analyzed in acquired digital images using ImageJ software (freely available from NIH) as described (Chang and Martin 2009).

Generating eGFP tg Mice without CyPD

Two different lines of mice with targeted deletions of both CyPD (*ppif*) alleles on different backgrounds were crossed to GlyT2-eGFP and Hb9-eGFP tg mice. Two different lines of CyPD null mice were used to rule out effects due to genetic strain. F1 offspring positive for the eGFP transgene and heterozygous knockout of CyPD were backcrossed with $ppif^{-/-}$ mice. The F2 generation therefore yielded progeny carrying all PCR-confirmed *ppif* genotypes ($CyPD^{+/+}$, $CyPD^{+/-}$, and $CyPD^{-/-}$) with or without the eGFP transgene. *ppif* deficiency was demonstrated by PCR identification of wild-type and targeted alleles from tail DNA and was confirmed by western blotting of biopsies of liver and skeletal muscle. GlyT2-eGFP; $CyPD^{-/-}$ and Hb9-eGFP; $CyPD^{-/-}$ mice were used for spinal cord injections of QA, KA, and PBS.

Results

QA and KA Induce Large-Scale Degeneration of Inter-neurons in Spinal Cord

After perfusion-fixation, each mouse spinal cord was examined for evidence of contusion and infarct. Only mice without evidence of contusion or infarct (Figure 1A) were analyzed further. Injection of PBS had no effect on neuronal number other than the damage caused at the injection needle track (Figure 1B, C). Injection of NMDA receptor agonist QA and non-NMDA receptor agonist KA directly into spinal cord parenchyma (Figure 1A, B) induced significant injury and degeneration of glycinergic interneurons in the ipsilateral side by 24 hours after micro-lesioning (Figure 1D–F). As determined by counting GlyT2-eGFP-positive interneurons in the intermediate zone of lumbar spinal cord, QA induced a loss of 80% ± 7% (mean ± *SD*) of glycinergic neurons (Figure 1D, F; Table 1), and KA induced a loss of 65% ± 9% of glycinergic interneurons (Figure 1E, F; Table 1).

Spinal Cord Interneurons Are More Sensitive than Motoneurons to NMDA Receptor- and Non-NMDA Receptor-Mediated Excitotoxicity

Lumbar spinal cord injection of QA and KA also induced significant degeneration of motoneurons by 24 hours after micro-lesioning (Figure 1G, H; Table 1). PBS injection had no effects on motoneuron number. As determined by counting Hb9-eGFP-positive motoneurons, QA induced a loss of 55% ± 6% (mean ± *SD*) of motoneurons, and KA induced a loss of 35% ± 4% of motoneurons in lumbar spinal cord (Figure 1F; Table 1).

Outcome after Spinal Cord Excitotoxicity Is Gender-Dependent

The effects of gender on CNS injury involving excitotoxic mechanisms are uncertain. Gender differences have been reported in experimental paradigms of spinal cord injury in adult mice where neurologic and neuropathologic outcomes were better in females than in

males (Farooque et al. 2006). However, studies of traumatic brain injury have found no significant gender effects (Bruce-Keller et al. 2007). With GlyT2-eGFP mice and Hb9-eGFP mice challenged in the spinal cord with excitotoxic agents, prominent gender effects were seen at whole animal (Figure 1I) and cellular levels. The mortality of male mice was ~80% when injected with 5.0 μmol QA (high dose) into lumbar spinal cord (Figure 1I), while nearly all female mice survived with this dose (Figure 1I). Overtly, the death seemed to be related to cardiorespiratory arrest. Mortality in male mice was reduced to 40% with injection of 2.5 μmol QA (Figure 1I), while all females survived (Figure 1I). At 24 hours after injection of 2.5 μmol QA into lumbar spinal cord, glycinergic interneuron loss was 77% ± 9% (mean ± *SD*) in male mice compared to 52% ± 7% loss in female mice.

Excitotoxic Degeneration of Spinal Interneurons Is Apoptotic while Spinal Motoneuron Degeneration Is Non-Apoptotic

Nissl staining of spinal cord sections from mice injected with PBS revealed normal cytology in the lumbar dorsal horn and intermediate zone (Figure 2A) and ventral horn (Figure 2B). In contrast, KA- and QA-injected mice had numerous apoptotic cells in dorsal horn and intermediate zone of spinal cord as evidenced by shrunken round profiles with dense chromatin masses (Figure 2C). Non-apoptotic neuronal degeneration was also seen, particularly in motoneurons (Figure 2D). Less apoptosis and apparently more necrotic cell death was seen with QA injection compared to KA injection into spinal cord (data not shown) consistent with our previous findings with QA injections into adult rat forebrain (Portera-Cailliau, Price, and Martin 1997b). It is critical to note that the presence of apoptotic and non-apoptotic neurodegeneration was independent of distance from the injection site as found earlier (Portera-Cailliau, Price, and Martin 1997a, 1997b). Morphological and immunohistochemical characteristics of cell death specifically in lumbar spinal cord interneurons and motoneurons were evaluated. In GlyT2-eGFP and Hb9-eGFP tg mice, the nucleus of eGFP-positive neurons is often seen as green due the high levels of transgene expression (Figure 3C–D) and can also be visualized as blue by counterstaining with Hoechst 33258. In degenerating GlyT2-eGFP interneurons, the nucleus and chromatin were condensed into sharply delineated, uniformly dense masses, which appeared as crescents abutting the nuclear envelope or as smooth, round masses within the nucleus (Figure 2E). Prominent alterations in the cytoplasm occurred concurrently with these changes in nuclear structure. The cytoplasm condensed and the cell shrunk in size and separated from the extracellular matrix (Figure 2E). Cleaved caspase-3 was detected in numerous degenerating GlyT2-eGFP interneurons (Figure 2F), but few caspase-3 positive neurons were detected in PBS-injected spinal cord; an occasional cell within or near the periventricular central canal was observed (data not shown). In contrast, Hb9-eGFP motoneurons undergoing NMDA receptor-mediated and non-NMDA receptor-mediated excitotoxicity had scant morphological features of apoptosis. Rather, these cells were typified by a pale nucleus with minimal chromatin condensation but extensive cytoplasmic disruption consistent with necrosis (Figure 2D). Another pattern of degeneration in motoneurons was the formation of many irregularly shaped, small chromatin clumps in the nucleus with a perikaryon that was less vacuolated than that seen in necrotic cell death (Figure 2G). Surprisingly, numerous non-apoptotically degenerating motoneurons in QA- and KA-injected mice were positive for cleaved caspase-3 (Figure 2H).

NMDA Receptor and Non-NMDA Receptor Stimulation Induces Changes in Mitochondrial Localization in Spinal Interneurons and Motoneurons

The mechanisms of excitotoxicity involve elevated intracellular Ca^{2+}, excessive production of nitric oxide and free radicals, and subsequent nitrosative and oxidative stress (Choi 1992; Carriedo et al. 1998; Martin 2002). In cultured neurons, this pathobiology can also influence mitochondrial morphology, trafficking, and the core regulators of mitochondrial fission and

fusion (Yuan et al. 2007; Reynolds et al. 2004). My laboratory tested the hypothesis that excitotoxicity causes mitochondrial fission *in vivo*. Spinal cord sections from GlyT2-eGFP transgenic mice injected with KA were immunolabeled for MnSOD and visualized for red fluorescent mitochondria (Figure 3A, B). Even at low magnifications, the colocalizations of green and red signals (seen as yellow) are more apparent in KA-injected mice (Figure 3B) compared to PBS-injected mice (Figure 3A). At 4 and 12 hours after KA injection, MnSOD-immunofluorescent mitochondria in interneurons were elevated dramatically compared to PBS-injected controls (Figure 3C, F). After QA injection, MnSOD-immunofluorescent mitochondria in interneurons were elevated significantly at 24 hours (Figure 3F). Mitochondria also accumulated in motoneurons after excitotoxin exposure, but the increase was less than that occurring in excitotoxically injured interneurons (data not shown). These changes occurred in neurons prior to changes in nuclear morphology indicative of degeneration (Figure 3D, E). At 24 hours after excitotoxin injection, cells at morphologically advanced stages of apoptotic or non-apoptotic stages of degeneration had lower amount of MnSOD-immunofluorescent mitochondria compared to controls (data not shown). Immunoperoxidase staining for MnSOD confirmed the excitotoxin-induced accumulation of mitochondria in neurons seen by fluorescent microscopy (Figure 3H, I).

ppif Gene Inactivation Blocks Apoptotic and Non-Apoptotic Neuronal Death Induced by Excitotoxicity

Excitotoxicitycan triggermitochondrial permeabilitytransition in cultured neurons (Reynolds et al. 2004; Yuan et al. 2007; Li, Brustovetsky, and Brustovetsky 2009). This study therefore determined if inactivation of the mPTP blocks spinal cord neuron cell death after excitotoxin exposure. Complete deletion of CyPD in $ppif^{-/-}$ mice significantly protected spinal cord neurons from excitotoxicity in two different mouse lines (Figure 3G; Table 1). Homozygous null inactivation of the *ppif* gene significantly rescued GlyT2-eGFP interneurons from QA and KA excitotoxicity (fewer neurons were lost compared to $ppif^{+/+}$ wild-type, Table 1, see also Figure 1F). The rescue of Hb9-eGFP motoneurons by *ppif* gene inactivation was also significant (the loss was only 15–30%, Table 1, $p < .05$, compare with Figure 1F) but less marked compared to the rescue of interneurons. CyPD deletion provided neuroprotection against apoptotic and non-apoptotic forms of neuronal cell death in spinal cord. CyPD deletion also attenuated the excitotoxin-induced accumulation of mitochondria in spinal cord neurons (Figure 3J).

Discussion

My laboratory used transgenic mice expressing eGFP in specific neuron types and a new mouse model of excitotoxic neuronal degeneration in spinal cord to uniquely examine *in vivo* the vulnerabilities of interneurons and motoneurons and their mechanisms of cell death involving mitochondria. This paradigm thus provides a specific example of an approach to study synaptic pathology and the endpoints to assess. The major findings in this study are (1) tg mice expressing eGFP in specific subsets of neurons are useful tools for delineating the responses of different types to neurons to neurotoxins because different types of neurons respond differently to toxic insults; (2) QA and KA microinjection into adult mouse spinal cord is a reliable and robust model for studying neuronal cell death and gender biases; (3) spinal interneurons are more vulnerable than spinal motoneurons to excitotoxicity; (4) spinal interneurons and spinal motoneurons undergoing excitotoxic degeneration die by different morphological processes involving apoptotic and non-apoptotic cell death, respectively; (5) neurons undergoing excitotoxic cell death accumulate mitochondria prior to the emergence of structural indications of cell death; and (6) apoptotic and non-apoptotic neuronal cell deaths *in vivo* are mediated by activation of the mPTP.

To harness transgenic mice that express eGFP in discrete subsets of neurons for use in a toxicologic paradigm, a new model needed to be developed. A perusal of the literature reveals that adult rats have been used in spinal cord excitotoxicity models (Magnuson et al. 1999; Hadi et al. 2000; Berens et al. 2005), but hitherto not mice. KA infusion into adult rat spinal cord induces lesions similar to contusion injuries (Magnuson et al. 1999). Moreover, large centrally placed KA injections into adult rat spinal cord can induce interneuron loss and paraplegia independent of motoneuron loss (Hadi et al. 2000). Our new model in adult mice requires careful stereotaxic microsurgery for successful implementation because of the potential ease of causing spinal cord traumatic injury unrelated to the excitotoxin injection. We found that microinjection of naturally occurring excitotoxins into spinal cord causes robust neurodegeneration. This approach is very reliable and has quantitative endpoints for assessing toxin-induced synaptic pathology and underlying molecular mechanisms. A very similar approach can be used to investigate excitotoxic synaptic mechanisms in cerebral cortex or hippocampus by using different transgenic mouse lines with fluorescent protein gene expression driven by different neuron-specific promoters.

An unanticipated outcome observed here was the prominent gender difference in vulnerability to the clinical consequences of intraparenchymal injection of excitotoxin into spinal cord. At equivalent doses of QA or KA, female mice always fared better than male mice at whole-animal and microscopic pathology levels. Our result is consistent with a previous report showing that adult female mice have better neurologic and neuropathologic outcomes than males after spinal cord traumatic injury (Farooque et al. 2006). The precise mechanisms contributing to the attenuated vulnerability of females are unknown but are likely to involve estrogen (Czlonkowska et al. 2005). Cell culture experiments have shown that estradiol can protect cultured embryonic rat spinal cord neurons (Nakamizo et al. 2000) and rat cortical neurons (Perrella and Bhavnani, 2005) from excitotoxicity, possibly by decreasing production of peroxynitrite (Perrella and Bhavnani 2005). The new *in vivo* mouse model of spinal cord excitotoxicity described here could be useful for delineating mechanisms of injury and preclinical therapeutic medicaments for acute (trauma) and chronic (multiple sclerosis and amyotrophic lateral sclerosis) neurological disorders involving degeneration of cells in the spinal cord and gender-based outcomes.

We found that glycinergic interneurons are more vulnerable than motoneurons to excitotoxicity. Interneuron networks in spinal cord control motoneuron activity (Rekling et al. 2000). Spinal interneurons can function as central pattern generators that sculpt, modulate, and drive patterns of motoneuron activity critical for voluntary limb and body movements as well as involuntary movements such as breathing (Rekling et al. 2000; Goulding 2009). Glycinergic synapses are abundant in spinal cord and brainstem (Jursky and Nelson 1995; Luque, Nelson, and Richards 1995). Four classes of genetically distinct interneuron pools (V0–V3) are derived from the embryonic ventral rhombencephalic neural tube, with each class exhibiting unique features (Goulding 2009). V0 interneurons are inhibitory, intersegmental, commissural neurons. V1 interneurons are inhibitory, with axons issuing rostroipsilaterally. V1 cells include the Renshaw cell and Ia inhibitory interneurons (Alvarez et al. 2005). V2 neurons project ipsilaterally and can be glutamatergic excitatory (V2a neurons) or inhibitory cells. V3 interneurons are excitatory commissural cells. A subset of the GlyT2-eGFP interneurons studied here are Renshaw cells, which can be identified unambiguously in adult mouse spinal cord by their size (small relative to other ventral interneurons), morphology, expression of glycinergic ($GlyT2^+$), and other markers (calbindin and nicotinic acetylcholine receptor $\alpha 2$), gephyrin clusters, location, and physiology (high postsynaptic sensitivity to acetylcholine and large glycine- and GABA-evoked currents (Alvarez and Fyffe 2007). Renshaw cells receive extensive cholinergic, glutamatergic (mediated by non-NMDA and NMDA receptors), GABAergic, and glycinergic inputs and exhibit vigorous, long-lasting, excitatory postsynaptic currents that

evoke high-frequency burst discharges with initial instantaneous frequencies of ~1,500 Hz (Eccles, Fatt, and Koketsu 1954; Mentis et al. 2006). Renshaw cells synapse directly on α-motoneurons, Ia inhibitory interneurons, and other Renshaw cells (Alvarez and Fyffe 2007; Eccles, Fatt, and Koketsu 1954). They account for 2–3% of all ventral interneurons in mouse spinal cord (Mentis et al. 2006). The Renshaw cell-to-motoneuron ratio is estimated to be 1:5 (Mentis et al. 2006). The intrinsic properties of interneurons are relatively different from motoneurons. Interneurons display high excitability with fast, repetitive, and prolonged action potential bursts; increased reliability of firing; high expression of Na^+ channels; high expression of Ca^{2+}-permeable AMPA receptors; spontaneous Ca^{2+} oscillations regulated by mitochondria; high oxidative metabolism; and substantial nitric oxide input (Alvarez and Fyffe 2007; Carr, Liu, and Zaruba 2001; Miles 2000). These intrinsic properties of glycinergic interneurons might render them more vulnerable than motoneurons to excitotoxicity.

Our excitotoxic model features spinal neuron degeneration by apparent apoptotic and non-apoptotic pathways in distinct populations of neurons. We have seen this before in a canine model of global cerebral ischemia (Martin, Sieber, and Traystman 2000). The neuronal apoptosis occurs discretely in subsets of interneurons and is homogeneous, precisely timed, and synchronous; thus, this model can be used to delineate cell death pathways in spinal interneurons destined to undergo unequivocal apoptosis as described for suprasegmental systems (Al-Abdulla and Martin 1998; Martin 2001; Martin, Kaiser, and Price 1999). The non-apoptotic cell death occurred in spinal motoneurons and had features consistent with necrotic cell death (Martin et al. 1998). We did not observe excitotoxically injured motoneurons degenerating with a morphology typical of apoptosis in this model. Another degenerative process observed in excitotoxically degenerating spinal motoneurons was a form intermediate between apoptosis and necrosis. This latter cell death morphology, seen in some motoneurons of KA-injected mice, is similar to the hybrid or continuum cell death that has been described previously as part of the apoptosis-necrosis cell death continuum (Portera-Cailliau, Price, and Martin 1997, 1997b; Martin 2002; Martin 2010) and possibly similar to necroptosis described more recently (Degterev et al. 2005). Consistent with the concept of the apoptosis-necrosis cell death continuum was the presence of non-apoptotically degenerating motoneurons positive for cleaved caspase-3. Thus, cleaved caspase-3 is not an unequivocal marker for neuronal apoptosis. Other studies have revealed that immunoreactivity for cleaved caspase-3 should not be equated with catalytically active enzyme because it can be present in apoptotically degenerating neurons without corresponding increases in activity (Lesuisse and Martin 2002) and can be present in non-apoptotically degenerating motoneurons without the formation of cleaved subunits of the appropriate molecular masses as shown by laser capture microdissection and mass spectroscopy (Martin et al. 2007).

This study shows that mitochondria accumulate in neurons destined for excitotoxic cell death *in vivo*. The mitochondrial accumulation in neurons occurred acutely (within 6 hours) at a time prior to morphological evidence for cell death. Possible explanations for the accumulation of perikaryal mitochondria in pre-apoptotic neurons are enhanced retrograde transport of mitochondria from dendrites and axons, decreased anterograde export of mitochondria to neuronal processes, or increased mitochondrial fission. We believe that the mitochondrial accumulation in excitotoxically stimulated spinal cord neurons is due to mitochondrial fission rather than other mechanisms. Currently this interpretation is based on the rapid timing of its occurrence. Mitochondrial accumulation due to trafficking perturbations requires at least 1 day (Al-Abdulla and Martin 1998; Martin et al. 2007). Experiments on cultured rat cortical neurons show that mitochondrial fission can occur within 1 hour of NMDA and nitric oxide exposure (Barsoum et al. 2006). Future experiments are needed on the molecular mechanisms of this mitochondrial accumulation to

support our interpretation regarding rapid mitochondrial fission in spinal cord neurons *in vivo* in response to excitotoxic stimulation.

We studied a possible mechanism through which mitochondria can mediate neurodegeneration *in vivo*. A direct role for mitochondria in the mechanisms of excitotoxic neuronal cell death in spinal cord was determined by investigating the mPTP. Mitochondrial permeability transition is a mitochondrial state in which the proton-motive force is disrupted reversibly or irreversibly (Rasola et al. 2010). Conditions of mitochondrial Ca^{2+} overload; excessive oxidative stress; and decreases in electrochemical gradient, ADP, and ATP can favor mitochondrial permeability transition (Crompton 1999; Bernardi et al. 2006; Halestrap 2009). This altered state of mitochondria involves the mPTP, which functions as a voltage, thiol, and Ca^{2+} sensor (Crompton 1999; Bernardi et al. 2006; Halestrap 2009). The mPTP is believed to be an inner mitochondrial membrane (IMM) high conductance channel or hemichannel (Rasola et al. 2010). The opening of this channel leads to permeabilization of the IMM to solutes <1,500 Da (Rasola et al. 2010). The collective components of the mPTP are not known. The voltage-dependent anion channel (VDAC) in the outer mitochondrial membrane (OMM), the adenine nucleotide translocator (ANT) in the IMM, and CyPD in the matrix have been implicated in mPTP functioning, yet they are each dispensable for the process of mitochondrial permeability transition (Rasola et al. 2010). CyPD is encoded by a single gene (*ppif*), and there is only one isoform of CyPD in humans and mice (Crompton 1999). The protein is a peptidyl-prolyl cis-trans isomerase (EC 5.2.1.8), which catalyzes the cis-trans isomerization of proline imidic peptide bonds in oligopeptides and accelerates the folding of proteins. CyPD binds ANT1 (Halestrap 2009). During normal mitochondrial function, the OMM and IMM are separated by the intermembrane space, and the VDAC and the ANT do not interact (Crompton 1999; Bernardi et al. 2006; Halestrap 2009). Permeability transition is activated by the formation of the mPTP as the IMM loses its integrity and the ANT changes conformation from its native state into a nonselective pore. This process is catalyzed by CyPD. When this occurs, small ions and metabolites permeate freely across the IMM, and oxidation of metabolites proceeds with electron flux not coupled to proton pumping, resulting in collapse of the electrochemical gradient, dissipation of ATP production, production of reactive oxygen species (ROS), equilibration of ions between the matrix and cytosol, matrix volume increases, and mitochondrial swelling (Crompton 1999; Bernardi et al. 2006; Halestrap 2009). We found that CyPD null mice were significantly less susceptible to excitotoxic neuronal cell death. This effect was robust in two different null lines on completely different genetic backgrounds, so the effect is not mouse strain dependent. Importantly, CyPD-deficient mice displayed a resistance to apoptotic and non-apoptotic neuronal cell deaths, as well as resistance to apparent mitochondrial fission, demonstrating for the first time that direct mitochondrial mechanisms involving CyPD regulate cell death independent of the ultimate structural phenotype of the neurodegeneration.

We conclude that mitochondria have a definite role in excitotoxic cell death mechanisms in spinal interneurons and motoneurons leading to their apoptotic or non-apoptotic degeneration mediated by the mPTP. Thus, the mPTP is likely to be an important mechanism-based target of pharmaceuticals designed as neuroprotectants with *in vivo* CNS efficacy. CyPD in particular appears to be an important target for neuroprotection therapies that can broadly affect neuronal cell death in general.

Acknowledgments

This work was supported by grants from the U.S. Public Health Service, NIH-NINDS (RO1-NS065895, RO1-NS052098) and NIH-NIA (RO1-AG016282).

The author thanks all of the individuals in his lab for their hard work, particularly Ann Price for the processing of the mouse spinal cords for histological assessments, Yan Pan for the mouse genotyping, and Margaret Wong for assistance with manuscript preparation. Special thanks are extended to Dr. Hanns Zeilhofer (Institute of Pharmacology and Toxicology, University of Zurich) for providing the original GlyT2-eGFP transgenic mice and Drs. Jeffery Molkentin (University of Cincinnati) and Michael Forte (Vollum Institute, Oregon Health and Science University) for providing the CyPD null mouse breeder pairs.

References

Aarts MM, Tymianski M. Molecular mechanisms underlying specificity of excitotoxic signaling in neurons. Curr Mol Med. 2004; 4:137–47. [PubMed: 15032710]

Al-Abdulla NA, Martin LJ. Apoptosis of retrogradely degenerating neurons occurs in association with the accumulation of perikaryal mitochondria and oxidative damage to the nucleus. Am J Pathol. 1998; 153:447–56. [PubMed: 9708805]

Alvarez FJ, Fyffe RE. The continuing case for the Renshaw cell. J Physiol. 2007; 584:31–45. [PubMed: 17640932]

Alvarez FJ, Jonas PC, Sapir T, Hartley R, Berrocal MC, Geiman EJ, Todd AJ, Goulding M. Postnatal phenotype and localization of spinal cord V1 derived interneurons. J Comp Neurol. 2005; 493:177–92. [PubMed: 16255029]

Arber S, Han B, Mendelsohn M, Smith M, Jessell TM, Sockanathan S. Requirement for the homeobox gene Hb9 in the consolidation of motor neuron identity. Neuron. 1999; 23:659–74. [PubMed: 10482234]

Auer, RN.; Benveniste, H. Hypoxia and related conditions. In: Graham, DI.; Lantos, PL., editors. Greenfield's Neuropathology. 6. Vol. 1. Oxford University Press; New York, NY: 1997. p. 263-314.

Baines CP, Kaiser RA, Purcell NH, Blair HS, Osinska H, Hambleton MA, Brunskill EW, Sayen MR, Gottlieb RA, Dorn GW, Robbins J, Molkentin JD. Loss of cyclophilin D reveals a critical role for mitochondrial permeability transition in cell death. Nature. 2005; 434:658–62. [PubMed: 15800627]

Barsoum MJ, Yuan H, Gerencser AA, Liot G, Kuchnareva YE, Gräber S, Kovacs I, Lee WD, Waggoner J, Cui J, White AD, Bossy B, Martinou JC, Youle RJ, Lipton SA, Ellisman MH, Perkins GA, Bossy-Wetzel E. Nitric oxide-induced mitochondrial fission is regulated by dynamin-related GTPases in neurons. EMBO J. 2006; 25:3900–11. [PubMed: 16874299]

Basso E, Fante L, Fowlkes J, Petronilli V, Fortes MA, Bernardi P. Properties of the permeability transition pore in mitochondria devoid of cyclophilin D. J Biol Chem. 2005; 280:18558–61. [PubMed: 15792954]

Berens SA, Colvin DC, Yu CG, Yezierski RP, Mareci TH. Evaluation of the pathologic characteristics of excitotoxic spinal cord injury with MR imaging. Am J Neuroradiol. 2005; 26:1612–22. [PubMed: 16091503]

Bernardi P, Krauskopf A, Basso E, Petronilli V, Blalchy-Dyson E, Di Lisa F, Forte MA. The mitochondrial permeability transition from *in vitro* artifact to disease target. FEBS J. 2006; 273:2077–99. [PubMed: 16649987]

Bruce-Keller AJ, Dimayuga FO, Reed JL, Wang C, Angers R, Wilson ME, Dimayuga VM, Scheff SW. Gender and estrogen manipulation do not affect traumatic brain injury in mice. J Neurotrauma. 2007; 24:203–15. [PubMed: 17263684]

Calhoun ME, Jucker M, Martin LJ, Thinakaran G, Price DL, Mouton PR. Comparative evaluation of synaptophysin-based methods for quantification of synapses. J Neurocytology. 1996; 25:821–28.

Carr PA, Liu M, Zaruba RA. Enzyme histochemical profile of immunohistochemically identified Renshaw cells in rat lumbar spinal cord. Brain Res Bull. 2001; 54:669–74. [PubMed: 11403994]

Carriedo SG, Yin HZ, Sensi SL, Weiss JH. Rapid Ca^{2+}-permeable AMPA/Kainate channels triggers marked intracellular Ca^{2+} rises and consequent oxygen radical production. J Neurosci. 1998; 18:7727–38. [PubMed: 9742143]

Chang Q, Martin LJ. Glycinergic innervation of motoneurons is deficient in amyotrophic lateral sclerosis mice: a confocal quantitative analysis. Am J Pathol. 2009; 174:574–85. [PubMed: 19116365]

Choi DW. Excitotoxic cell death. J Neurobiol. 1992; 23:1261–76. [PubMed: 1361523]

Clements JD, Lester RAJ, Tong G, Jahr CE, Westbrook GL. The time course of glutamate in the synaptic cleft. Science. 1992; 258:1498–1501. [PubMed: 1359647]

Collingridge GL, Olsen RW, Peters J, Spedding M. A nomenclature for ligand-gated ion channels. Neuropharmacology. 2009; 56:2–5. [PubMed: 18655795]

Crompton M. The mitochondrial permeability transition pore and its role in cell death. Biochem J. 1999; 341:233–49. [PubMed: 10393078]

Curtis DR, Phillis JW, Watkins JC. Chemical excitation of spinal neurons. Nature. 1959; 183:611–12. [PubMed: 13632811]

Czlonkowska A, Ciesielska A, Gromadzka G, Kurkowska-Jastrzebska I. Estrogen and cytokines production—the possible cause of gender differences in neurological diseases. Curr Pharm Des. 2005; 11:1017–30. [PubMed: 15777251]

Degterev A, Huang Z, Boyce M, Li Y, Jagtap P, Mizushima N, Cuny GD, Michitson TJ, Moskowitz MA, Yuan J. Chemical inhibitor of nonapoptotic cell death with therapeutic potential for ischemic brain injury. Nat Chem Biol. 2005; 1:112–19. [PubMed: 16408008]

Eccles JC, Fatt P, Koketsu K. Cholinergic and inhibitory synapses in a pathway from motor-axon collaterals to motoneurons. J Physiol. 1954; 126:524–62. [PubMed: 13222354]

Farooque M, Suo Z, Arnold PM, Wulser MJ, Chou CT, Vancura RW, Fowler S, Festoff BW. Gender-related differences in recovery of locomotor function after spinal cord injury in mice. Spinal Cord. 2006; 44:182–87. [PubMed: 16130019]

Ginsberg, SD.; Hemby, SE.; Mufson, EJ.; Martin, LJ. Cell and tissue microdissection in combination with genomic and proteomic profiling. In: Zaborszky, L.; Wouterlood, FG.; Lanciego, JL., editors. Neuroanatomical Tract-Tracing 3. Molecules, Neurons, and Systems. Springer; New York, NY: 2006. p. 109-41.

Goulding M. Circuits controlling vertebrate locomotion: Moving in a new direction. Nat Rev. 2009; 10:507–18.

Hadi B, Zhang YP, Burke DA, Shields CB, Magnuson SK. Lasting paraplegia caused by loss of lumbar spinal cord interneurons in rats: no direct correlation with motor neuron loss. J Neurosurg (Spine 2). 2000; 93:266–75.

Halestrap AP. What is the mitochondrial permeability transition pore? J Mol Cell Cardiol. 2009; 46:821–31. [PubMed: 19265700]

Jursky F, Nelson N. Localization of glycine neurotransmitter transporter (GLYT2). reveals correlation with the distribution of glycine receptor. J Neurochem. 1995; 64:1026–33. [PubMed: 7861131]

Lesuisse C, Martin LJ. Immature and mature cortical neurons engage different apoptotic mechanisms involving caspase-3 and the MAP kinase pathway. J Cereb Blood Flow Metabol. 2002; 22:935–50.

Li V, Brustovetsky T, Brustovetsky N. Role of cyclophilin D-dependent mitochondrial permeability transition in glutamate-induced calcium deregulation and excitotoxic neuronal death. Exp Neurol. 2009; 218:171–82. [PubMed: 19236863]

Lok J, Martin LJ. Rapid suncellular redistribution of Bax precedes caspase-3 and endonuclease activation during excitotoxic neuronal apoptosis in rat brain. J Neurotrauma. 2002; 19:815–28. [PubMed: 12184852]

Lucas DR, Newhouse JP. The toxic effect of sodium *L*-glutamate on the inner layers of the retina. AMA Arch Opthalmol. 1957; 58:193–201.

Luque JM, Nelson N, Richards JG. Cellular expression of glycine transporter 2 messenger RNA exclusively in rat hindbrain and spinal cord. Neuroscience. 1995; 64:525–35. [PubMed: 7700536]

Magnuson DSK, Trinder TC, Zhang YP, Burke D, Morassutti DJ, Shields CB. Comparing deficits following excitotoxic and contusion injuries in the thoracic and lumbar spinal cord of the adult rat. Exp Neurol. 1999; 156:191–204. [PubMed: 10192790]

Malouitre S, Dube H, Selwood D, Crompton M. Mitochondrial targeting of cyclosporine A enables selective inhibition of cyclophilin-D and enhanced cytoprotection after glucose and oxygen deprivation. Biochem J. 2010; 425:137–48. [PubMed: 19832699]

Martin LJ. Neuronal cell death in nervous system development, disease, and injury. Int J Mol Med. 2001; 7:455–78. [PubMed: 11295106]

Martin, LJ. Neurodegenerative disorders of the human brain and spinal cord. In: Ramachandran, VS., editor. Encyclopedia of the Human Brain. Vol. 3. Elsevier Science; Amsterdam: 2002. p. 441-63.

Martin LJ. Mitochondrial and cell death mechanisms in neurodegenerative diseases. Pharmaceuticals. 2010; 3:839–915. [PubMed: 21258649]

Martin LJ, Al-Abdulla NA, Brambrink AM, Kirsch JR, Sieber FE, Portera-Cailliau C. Neurodegeneration in excitotoxicity, global cerebral ischemia, and target deprivation: A perspective on the contributions of apoptosis and necrosis. Brain Res Bull. 1998; 46:281–309. [PubMed: 9671259]

Martin LJ, Kaiser A, Price AC. Motor neuron degeneration after sciatic nerve avulsion in adult rat evolves with oxidative stress and is apoptosis. J Neurobiol. 1999; 40:185–201. [PubMed: 10413449]

Martin LJ, Liu Z, Chen K, Price AC, Pan Y, Swaby JA, Golden WC. Motor neuron degeneration in amyotrophic lateral sclerosis mutant superoxide dismutase-1 transgenic mice: Mechanisms of mitochondriopathy and cell death. J Comp Neurol. 2007; 500:20–46. [PubMed: 17099894]

Martin LJ, Pardo CA, Cork LC, Price DL. Synaptic pathology and glial responses to neuronal injury precede the formation of senile plaques and amyloid deposits in the aging cerebral cortex. Am J Pathol. 1994; 145:1358–81. [PubMed: 7992840]

Martin LJ, Sieber FE, Traystman RJ. Apoptosis and necrosis occur in separate neuronal populations in hippocampus and cerebellum after ischemia and are associated with differential alterations in metabotropic glutamate receptor signaling pathways. J Cereb Blood Flow Metab. 2000; 20:153–67. [PubMed: 10616804]

Martin LJ, Gertz B, Pan Y, Price AC, Molkentin JD, Chang Q. The mitochondrial permeability transition pore in motor neurons: Involvement in the pathobiology of ALS mice. Exp Neurol. 2009; 218:333–46. [PubMed: 19272377]

Mentis GZ, Siembab VC, Zerda R, O'Donovan MJ, Alvarez FJ. Primary afferent synapses on developing and adult Renshaw cells. J Neurosci. 2006; 26:13297–310. [PubMed: 17182780]

Miles R. Diversity of inhibition. Science. 2000; 287:244–46. [PubMed: 10660424]

Nakamizo T, Urushitani M, Inoue R, Shinohara A, Sawada H, Honda K, Kihara T, Akaike A, Shimohama S. Protection of cultured spinal motor neurons by estradiol. Neuroreport. 2000; 11:3493–97. [PubMed: 11095506]

Nakanishi S. Molecular diversity of glutamate receptors and implications for brain function. Science. 1992; 258:597–603. [PubMed: 1329206]

Nguyen KT, Garcia-Chacon LE, Barrett JN, Barrett EF, David G. The ψ_m depolarization that accompanies mitochondrial Ca^{2+} uptake is greater in mutant SOD1 than in wild-type mouse motor terminals. Proc Natl Acad Sci USA. 2009; 106:2007–11. [PubMed: 19174508]

Okabe M, Ikawa M, Kominami K, Nakanishi T, Nishimune Y. "Green mice" as a source of ubiquitous green cells. FEBS Lett. 1997; 407:313–19. [PubMed: 9175875]

Oliva AA, Jiang M, Lam T, Smith KL, Swann JW. Novel hippocampal interneuronal subtypes identified using transgenic mice that express green fluorescent protein in GABAergic interneurons. J Neurosci. 2000; 20:3354–68. [PubMed: 10777798]

Olney JW. Excitatory transmitter neurotoxicity. Neurobiol Aging. 1994; 15:259–60. [PubMed: 7838306]

Perrella J, Bhavnani B. Protection of cortical cells by equine estrogens against glutamate-induced excitotoxicity is mediated through a calcium independent mechanism. BMC Neurosci. 2005; 6:34–51. [PubMed: 15882473]

Peters, A.; Palay, SL.; Webster, HD. The Fine Structure of the Nervous System: Neurons and Their Supporting Cells. Oxford University Press; New York, NY: 1991.

Portera–Cailliau C, Price DL, Martin LJ. Excitotoxic neuronal death in the immature brain is an apoptosis–necrosis morphological continuum. J Comp Neurol. 1997a; 378:70–87.

Portera–Cailliau C, Price DL, Martin LJ. Non–NMDA and NMDA receptor–mediated excitotoxic neuronal deaths in adult brain are morphologically distinct: further evidence for an apoptosis–necrosis continuum. J Comp Neurol. 1997b; 378:88–104.

Rasola A, Sciacovelli M, Pantic B, Bernardi P. Signal transduction to the permeability transition pore. FEBS Lett. 2010; 584:1989–96. [PubMed: 20153328]

Rekling JC, Funk GD, Bayliss DA, Dong XW, Feldman JL. Synaptic control of motoneuronal excitability. Physiol Rev. 2000; 80:767–852. [PubMed: 10747207]

Reynolds IJ, Malaiyandi LM, Coash M, Rintoul GL. Mitochondrial trafficking in neurons: a key variable in neurodegeneration? J Bioenerg Biomembr. 2004; 36:283–86. [PubMed: 15377858]

Seeburg PH. The molecular biology of mammalian glutamate receptor channels. TINS. 1993; 16:359–65. [PubMed: 7694406]

Siddiqui AH, Joseph SA. CA3 axonal sprouting in kainite-induced chronic epilepsy. Brain Res. 2005; 1066:129–46. [PubMed: 16359649]

Skirboll, LA.; Thor, K.; Helke, C.; Hokfelt, T.; Robertson, B.; Long, R. Use of retrograde fluorescent tracers in combination with immunohistochemical methods. In: Heimer, L.; Zaborszky, L., editors. Neuroanatomical Tract-Tracing Methods 2. Plenum; New York, NY: 1989. p. 5-18.

Sotelo, C.; Triller, A. The central neuron. In: Graham, DI.; Lantos, PL., editors. Greenfield's Neuropathology. 6. Vol. 1. Oxford University Press; New York, NY: 1997. p. 3-61.

Stewart GR, Zorumski CF, Price MT, Olney JW. Domoic acid: A dementia-inducing excitotoxic food poison with kainic acid receptor specificity. Exp Neurol. 1990; 110:127–38. [PubMed: 2170163]

Stone BS, Zhang J, Mack DW, Mori S, Martin LJ, Northington FJ. Delayed neural network degeneration after neonatal hypoxia-ischemia. Ann Neurol. 2008; 64:535–46. [PubMed: 19067347]

Sudhof TC. The synaptic vesicle cycle: A cascade of protein-protein interactions. Nature. 1995; 375:645–53. [PubMed: 7791897]

Thaler J, Harrison K, Sharma K, Lettieri K, Kehrl J, Pfaff SL. Active suppression of interneuron programs within developing motor neurons revealed by analysis of homeodomain factor HB9. Neuron. 1999; 23:675–87. [PubMed: 10482235]

Verity, MA. Toxic disorders. In: Graham, DI.; Lantos, PL., editors. Greenfield's Neuropathology. 6. Vol. 1. Oxford University Press; New York NY: 1997. p. 755-811.

Watkins JC, Evans RH. Excitatory amino acid transmitters. Ann Rev Pharmcol Toxicol. 1981; 21:165–204.

Wichterle H, Lieberam I, Porter JA, Jessell TM. Directed differentiation of embryonic stem cells into motor neurons. Cell. 2002; 110:385–97. [PubMed: 12176325]

Yang ZJ, Carter EL, Torbet MT, Martin LJ, Koehler RC. Sigma receptor ligand 4-phenyl-1-(4-phenylbutyl).-piperidine modulates neuronal nitric oxide synthase/postsynaptic density-95 coupling mechanisms and protects against neonatal ischemic degeneration of striatal neurons. Exp Neurol. 2010; 221:166–74. [PubMed: 19883643]

Yuan H, Gerencser AA, Liot SA, Ellisman M, Perkins GA, Bossy-Wetzel E. Mitochondrial fission is an upstream and required event for bax foci formation in response to nitric oxide in cortical neurons. Cell Death Differ. 2007; 14:462–71. [PubMed: 17053808]

Zeilhofer HU, Studler B, Arabadzisz D, Schweizer C, Ahmadi S, Layh B, Bosl MR, Fritschy JM. Glycinergic neurons expressing enhanced green fluorescent protein in bacterial artificial chromosome transgenic mice. J Comp Neurol. 2005; 482:123–41. [PubMed: 15611994]

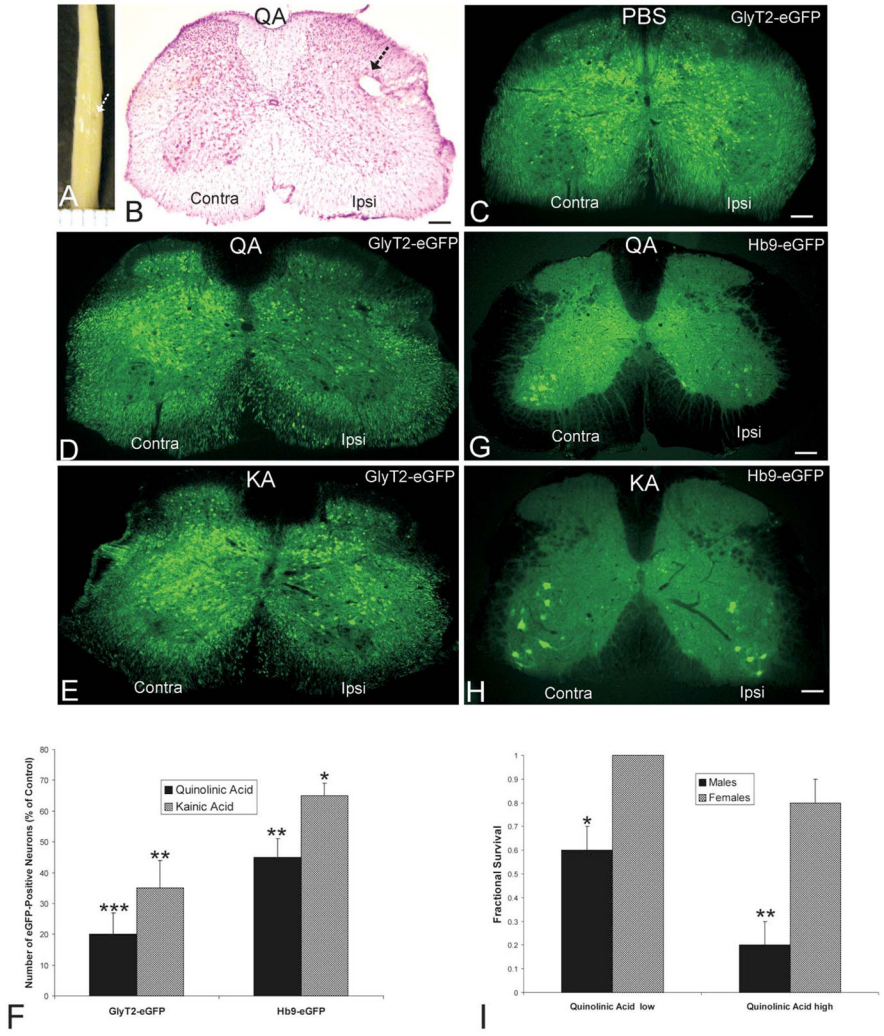

Figure 1.

Excitotoxin micro-injection into adult mouse spinal cord induces interneuron and motoneuron degeneration. **A.** Mouse spinal cord after stereotaxic unilateral injection (arrow) of the NMDA receptor agonist quinolinic acid (QA) into lumbar spinal cord and survival for 24 hours. Ruler lines at bottom are 1 mm apart. **B.** Lumbar spinal cord section from a female GlyT2-eGFP tg mouse at 24 hours after unilateral injection of QA (5.0 μmol, 1 μl). The section (40 μm thick) is stained with cresyl violet (Nissl stain) and shows the injection site (arrow) and the loss of cells in the side ipsilateral (Ipsi) to the injection compared to the noninjected contralateral (Contra) side. Scale bar = 130 μm. **C.** Lumbar spinal cord section from a female GlyT2-eGFP tg mouse at 24 hours after unilateral injection of PBS. The glycinergic interneurons are green. Ipsilateral and contralateral sides have similar numbers of green neurons. Scale bar = 130 μm (same for D and E). **D and E.** Lumbar spinal cord section from female GlyT2-eGFP tg mice at 24 hours after unilateral injection of QA (5.0 μmol, 1 μl) or kainic acid (KA) (400 μmol, 1 μl). The glycinergic interneurons are green. The ipsilateral sides have reduced numbers of green neurons compared to the contralateral sides. QA induces more severe loss of glycinergic interneurons. **F.** Graph showing the number of glycinergic interneurons ipsilaterally in the lumbar spinal cord of female GlyT2-eGFP tg mice or HB9-eGFP tg mice at 24 hours after unilateral injection of QA or KA relative to PBS-injected controls. The values are mean ± *SD* for 6 mice per group.

Significant differences are indicated by asterisks (*$p < .05$, **$p < .01$, ***$p < .005$). **G and H.** Lumbar spinal cord section from female Hb9-eGFP tg mice at 24 hours after unilateral injection of QA (5.0 μmol, 1 μl) or KA (400 μmol, 1 μl). The motoneurons are green. The ipsilateral sides have reduced numbers of green neurons compared to the contralateral sides. QA induces more severe loss of motoneurons (see F for cell counts). Scale bars = 120 μm (G) and 110 μm (H). **I.** Graph showing the survival of male and female mice injected unilaterally into lumbar spinal cord with 1μl of 5.0 μmol (high) or 2.5 μmol (low) QA. The experiment was done in duplicate with ten mice in each group. The values are mean ± *SD*. Significant differences are indicated by asterisks (*$p < .01$, **$p < .005$).

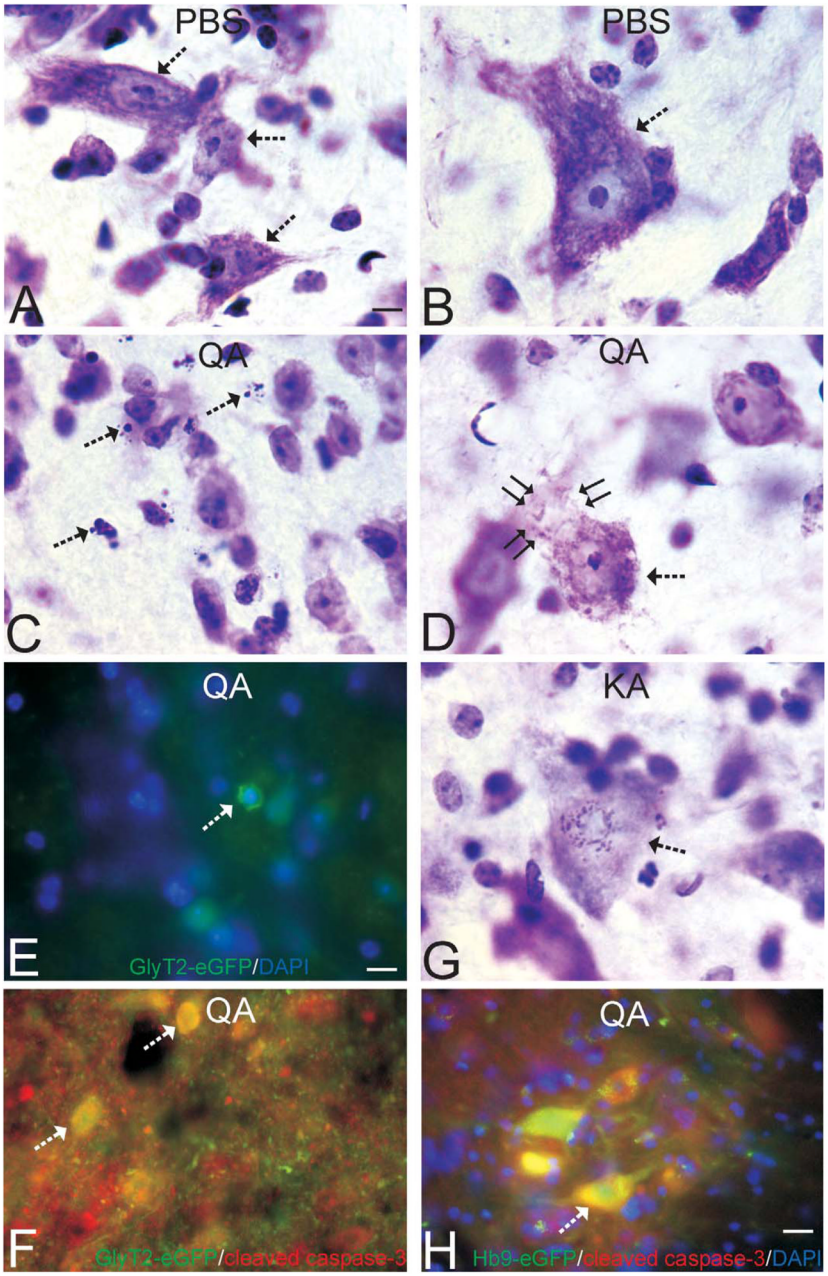

Figure 2.

Cytology of excitotoxic neurodegeneration in adult mouse spinal cord. **A and B.** PBS micro-injection did not cause neurodegeneration of putative interneurons in the intermediate zone (A, arrows) or motoneurons in ventral horn (B, arrow) as shown by Nissl staining. Scale bar = 8 μm (same for B–D, G). **C and D.** Quinolinic acid (QA, 5.0 μmol, 1 μl) micro-injection induced robust neurodegeneration of putative interneurons in the intermediate zone (C, arrows) and motoneurons in ventral horn (D, arrow) by 24 hours as shown by Nissl staining. In the intermediate zone of spinal cord, numerous end-stage apoptotic profiles were observed (C, arrows). Motoneuron degeneration was necrotic-like with dissipation of the nuclear matrix and cytoplasmic vacuolar changes. The large perikaryon and broad proximal dendrites showed severely diminished Nissl staining with the formation of large vacuoles

(D, double arrows). **E.** Quinolinic acid (QA) (5.0 μmol, 1 μl) induced apoptosis of glycinergic interneurons in GlyT2-eGFP transgenic mice. The shrunken glycinergic interneuron (seen as green, arrow) has its DNA packaged into a large condensed mass as seen by the blue Hoechst 33258 dye staining. Other nuclei of surrounding neurons and glia are seen as blue without green. Scale bar = 9 μm (same for F, H). **F.** After QA injection (5.0 μmol, 1 μl), degenerating glycinergic interneurons were positive for cleaved caspase-3 (arrows). Yellow represents the colocalization of green (eGFP) and red (cleaved caspase-3 immunoreactivity). **G.** In mice with kainic acid (KA) (400 μmol, 1 μl) micro-injection into spinal cord, the degenerating motoneurons (arrow) often appeared with many small clumps of chromatin within the nucleus and the attenuation of Nissl staining was less severe compared to motoneurons with more necrotic-like morphologies seen with QA. **H.** After QA injection (5.0 μmol, 1 μl), degenerating motoneurons were positive for cleaved caspase-3 (arrow), despite the non-apoptotic degeneration morphology. Yellow represents the colocalization of green (eGFP) and red (cleaved caspase-3 immunoreactivity). Nuclei of surrounding neurons and glia are seen as blue.

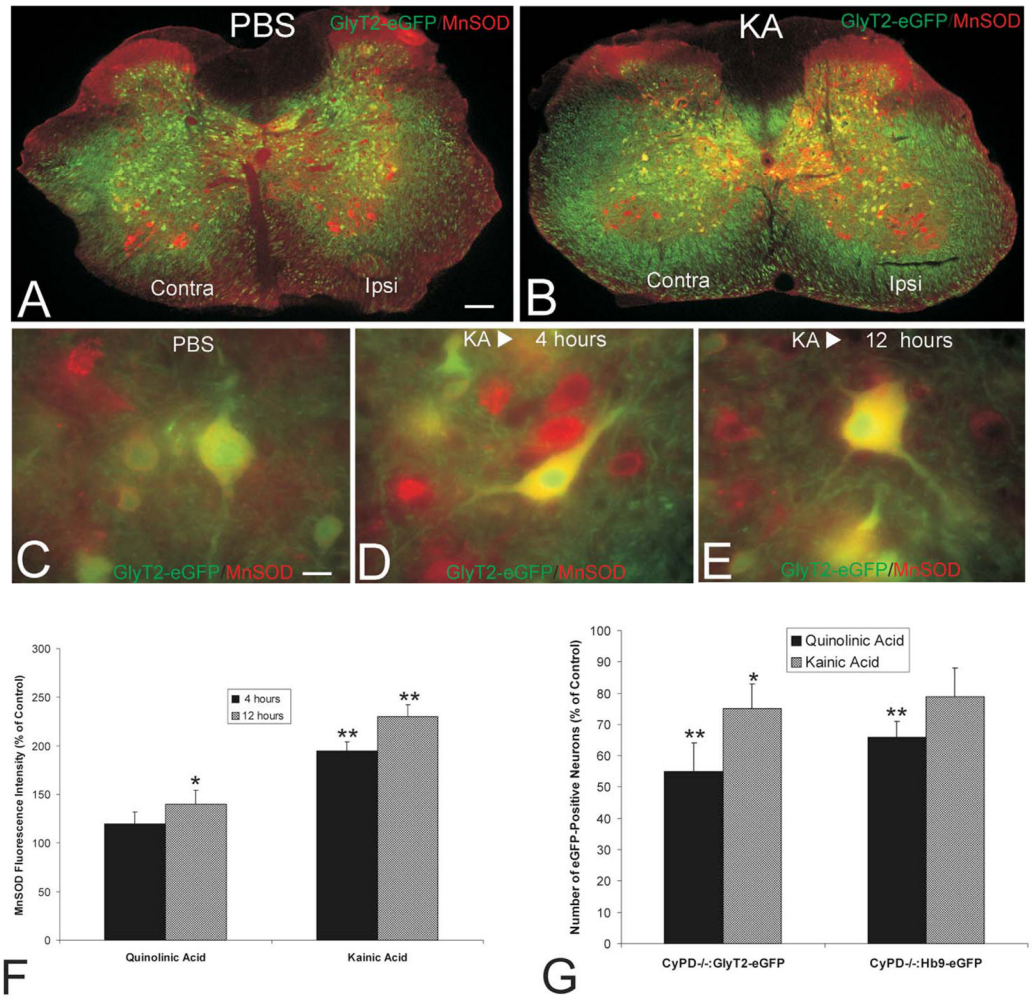

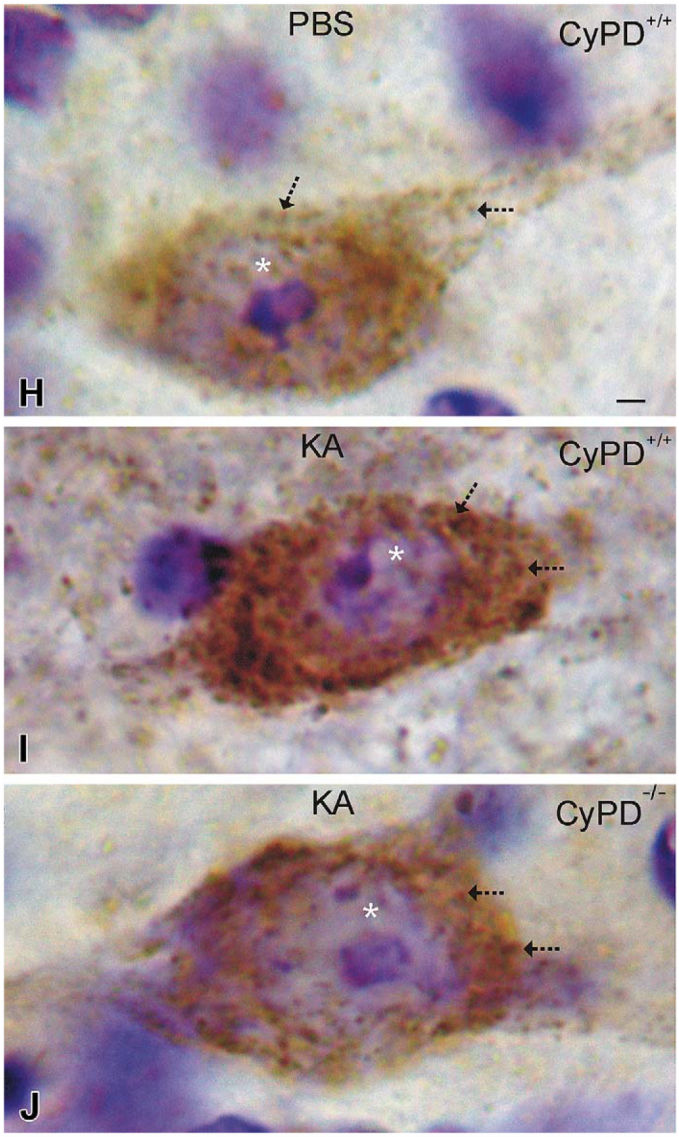

Figure 3.

Interneurons undergoing excitotoxic degeneration accumulate mitochondria and die through mitochondrial permeability transition pore (mPTP)-regulated cell death mechanisms. **A and B.** Low-magnification images of lumbar spinal cord sections from PBS-injected (A) or kainic acid (KA)–injected GlyT2-eGFP tg mice showing the distributions of eGFP (green) and the mitochondrial marker manganese superoxide dismutase (MnSOD, red). Yellow indicates colocalization of green and red. The intensified yellow signal in the KA-injected mouse spinal cord indicates the accumulation of mitochondria in glycinergic interneurons. **C–E.** Glycinergic interneurons in spinal cord of mice injected with PBS (C) have low MnSOD mitochondrial staining compared to glycinergic interneurons in spinal cord of mice injected with KA that show dramatic elevation of mitochondrial staining at 4 hours (D) and 12 hours (E) after KA exposure. F. Graph showing fluorescence intensity signal for mitochondria in glycinergic interneurons in lumbar spinal cord of GlyT2-eGFP tg female mice injected with quinolinic acid (QA, 5.0 μmol), KA (400 μmol), or PBS (controls). The values are mean ± *SD* of six mice per group and counts of ~25 neurons per mouse. Significant differences are indicated by asterisks (*$p < .05$, **$p < .001$). **G.** Graph showing

the number of glycinergic interneurons and motoneurons at 24 hours after spinal cord injection of QA or KA in GlyT2-eGFP;CyPD$^{-/-}$ and Hb9-eGFP;-CyPD$^{-/-}$ mice (compare with Figure 1F). This data set is on the C57BL/6 CyPD null background. Values are mean ± *SD* (*n* = 6–10 mice per genotype). Significant differences compared to eGFP wild-type, PBS-injected mice are indicated by asterisks (*$p < .05$, **$p < .01$). **H–J.** Immunoperoxidase staining for MnSOD in putative spinal cord interneurons (based on size, morphology, and location) in GlyT2-eGFP;CyPD$^{+/+}$ and GlyT2-eGFP;CyPD$^{-/-}$ mice at 6 hours after spinal cord injection of PBS or KA. Scale bar in H = 3.3 μm (applies to I & J). Immunoreactive mitochondria are seen as discrete puncta or larger aggregates (arrows) within the neuronal cytoplasm. The sections have been counterstained with cresyl violet, so the nucleolus and chromatin appear violet within the nucleus (asterisk). KA induced dramatic accumulation of mitochondria in the neuronal cell body (I) compared to neurons in PBS-injected spinal cord (H). Inactivation of the mPTP by CyPD deletion attenuated the mitochondrial accumulation in spinal cord neurons after KA (J).

Table 1

Excitotoxic Degeneration of Spinal Interneurons and Motoneurons Is Gender-Dependent and Regulated by Cyclophilin D

	Number of neurons (% of vehicle control)			
	Quinolinic Acid (5.0 μmol)		Kainic Acid (400 μmol)	
Genotype	**Male (*N* = 4)**	**Female (*N* = 6)**	**Male (*N* = 4)**	**Female (*N* = 6)**
GlyT2-eGFP;CyPD$^{+/+}$	10 ± 6***	20 ± 7***	25 ± 5***	35 ± 7**
Hb9-eGFP;CyPD$^{+/+}$	34 ± 4**	45 ± 6**	53 ± 6**	65 ± 4*
GlyT2-eGFP;CyPD$^{-/-}$	46 ± 10^{++}	55 ± 9^{++}	54 ± 9^{++}	75 ± 8^{+}
Hb9-eGFP;CyPD$^{-/-}$	55 ± 11^{++}	66 ± 6^{+}	63 ± 11^{+}	79 ± 9

Values are mean ± *SD*.

*** $p < .001$.

** $p < .005$.

* $p < .01$.

$^{++}$ $p < .01$.

$^{+}$ $p < .05$.